Electronic Supplementary Material (ESI) for Molecular BioSystems.

Molecular dynamics simulations and in vitro analysis of the CRMP2 thiol switch

Daniel Möller[+1], Manuela Gellert[+2], Walter Langel[1], Christopher Horst Lillig*[2]

[+] These authors contributed equally to this work.

* corresponding author: horst@lillig.de

[1] Biophysical Chemistry, Institute of Biochemistry, University Greifswald, 17489 Greifswald, Germany

[2] Institute for Medical Biochemistry and Molecular Biology, University Medicine, University Greifswald, 17489 Greifswald, Germany

Supporting Information

Methods

Homology search

The most complete experimental structure 2VM8 covers 477 amino acids from Ser14 to Glu490[1]. For our study, the N-terminus was not relevant, and we omitted the first 15 aa up to Arg16. This structure still lacks the C-terminal residues 491-577, which include the major regulatory and phosphorylation sites of the protein[2-4]. We thus had to extend the structure by *in silico* methods up to the postulated cleavage site of the protease calpain, i.e. by 41 amino acids (Lys491 - Val531) with the sequence LRGVPRGLYDGPVCEVSVTPKTVTPASSAKTSPAKQQAPPV. Marked are Cys504 in red for the dithiol-disulphide redox switch; Thr509, Thr514, Ser517, Ser518 and Ser522 in brown as phosphorylation sites; and the calpain cleavage site highlighted in grey. By homology search (SWISS-Model[5-8]), we only found a template structure for the next nine aa Lys491-Tyr499 in human dihydropyrimidinase (Q14117) with the structure 2VR2[9].

Force-field package, REMD algorithm and solvent models

We now had a structure for Arg16 to Tyr499. For further simulations, a structure model covering the next 32 aa at the C-terminus till residue 531 was necessary and we used different kinds of force field based molecular dynamics (MD) to predict *in silico* the structure of the remaining 32 aa (Asp500 to Val531). Geometry optimization and molecular dynamics simulations were done using the NAMD package[10] with the AMBER-force field (ff14SB)[11,12]. For the short-range non-bonded interaction, van der Waals and electrostatic interactions were calculated until a 10 Å direct-space cut-off including a smoothing function for the potentials. Particle Mesh Ewald (PME) was used for the long-range electrostatics under periodic boundary conditions. Energy minimization was achieved by a conjugate gradient and line search algorithm in NAMD.

In MD simulations, all covalent bonds to hydrogen atoms were constrained to their nominal lengths by the RATTLE algorithm. Molecular dynamics applied a Verlet integrator with a dual time step of 2 fs for the bonded and van der Waals interactions and 4 fs for PME. A Langevin thermostat was used with a damping time every 1 ps in NVT (constant particle **N**umber, cell **V**olume and **T**emperature of 300 K) and NPT (constant **P**ressure of 1 bar) or every 100 ps in NVE (constant **E**nergy) calculations. The NPT protocol used a Langevin piston constant pressure control[13,14] with an oscillation period of 200 fs and a damping time of 100 fs in combination with a thermostat. The AMBER-tool xleap was used to build the systems via ion solvation and positioning. The visualization package VMD was used with its plugins[15-21]

to analyse secondary structure (STRIDE), electrostatic potentials (PME), SASA and radius of gyration of the simulated structures.

Protein folding in implicit and explicit solvent

The sequence of 32 amino acids had acetyl and N-methyl protection groups at its N- and C-termini, respectively. Two different secondary starting structures were generated, one strand and an α helix. Thereby, we wanted to avoid that the result for folding were dominated by our starting g structure. We used both implicit solvent (GBSA)[22-25] and explicit water (TIP3P-water model for force field)[26] as solvents respectively.

A replica exchange molecular dynamics approach was used to accelerate the search for an initial C-terminal structure, corresponding to previous results with a larger helical portion[2]. The Boltzmann ensemble and the energy surface map of the molecules was generated by replica-exchange MD (REMD) [27,28] algorithms. With this approach we overcame the energy barriers between folding states without the generation of a full Boltzmann ensemble. We minimized the box size of the extended protein to a more compact size with implicit solvent conditions. Following REMD algorithms in discrete water produced folded proteins and helical parts in the extended amino acid chain. However, the termini were not accessible to form a bond with the CRMP2 body and also the position of the Cys504 residue was compromised averting disulphide bond formation. Therefore we used a different structure of the peptide with accessible N-terminus for a connection with the CRMP2 body. A third REMD was performed at the surface of the CRMP2 (**Figure SI 1**.B) with spatial restriction to the Cys504, which allowed disulphide bond formation.

REMD in implicit water

We started with a REMD [27,28] algorithm to relax the structures and to generate first folds of the aa chain. In a classical REMD an exchange between two replicas at nearby temperatures with a similar potential energy is triggered by fulfilling the Metropolis criterion. Our system contained twelve replica over a temperature range of 270 to 700 K. This number of replica is sufficient for the distributions of potential energies of replica at neighbouring temperatures, to achieve their overlapping facilitating a significant probability of exchange. The calculation was accelerated by omitting the solvent molecules and counter ions as well as by working in implicit solvent (GBSA). Each replica contained only the 461 atoms of the peptide.

Verification of exchange was done in intervals of 1 ps. After 100 ns all replicas had frequently switched between different structures even at low temperatures. The folding in implicit water only attained conformations with a small number of secondary structure elements[29]. We used the results as initial configuration for simulations in explicit water.

TIGER2 with explicit water

We switched to the recently developed TIGER2 (temperature intervals with global exchange of replicas) algorithm[30,31]. In contrast to standard REMD, all replica are cooled down to the basis temperature before verifying an exchange, which minimizes the influence of temperature on the potential energy in favour of structural differences. Consequently, a smaller number of replica is needed compared to standard REMD, and the calculation is better adapted to the hardware. All further simulations ran under periodic boundary conditions with TIP3P-water as explicit solvent. In explicit solvent, the temperature range is limited to 280 to 600 K. The TIGER2-algorithm was customized combining pressure control[13,14] with explicit solvent as NPT simulations. The set point of the pressure was chosen to be significantly higher than the respective vapour pressure of the solvent avoiding partial evaporation of the water and bubbles. The two replicas, one from strand (now 7008 atoms including 2182 water molecules) and one from helical starting structures (now 7479 atoms including 2339 water molecules), were taken as initial structures for two TIGER2 simulations. Booth structures had the most secondary structure elements and hydrogen bonds at the end of the two implicit solvent calculations. Each of these two optimized structures gave rise to twelve replica, with a simulation time 500 ns each. The Metropolis criterion was applied each 2 ps. The overall charge of the peptide is +1 e (e is the positive elementary charge), which was compensated by one Cl^-. For the following simulations, we chose the structure among the 24 with the highest amount of (helical) secondary structure elements and highest count of hydrogen bonds and an accessible N-terminus.

Folding at the protein surface

We connected the residue Asp500 of the final structure from the TIGER2 runs with the residue Tyr499 of the homology search structure and got a peptide of 41 amino acids (Lys491-Val531), which is linked to the body of the CRMP2 monomer (chain A) at the residue 490 of the C-terminus. We cut this structure maintaining only the residues neighbouring to the new C-terminus (**Figure SI 1.B**). The C_α atoms of the CRMP2 main body were fixed during further calculations, in order to conserve the natural environment of the C-terminus.

Following energy minimization, we equilibrated the system during three simulations at 300 K. We used the protocol NVT (1 ns), NVP (0.5 ns) and NVT (1 ns) for equilibration of the system, followed by 6 ns NVE. The resulting structure was subjected to a second TIGER2-NPT simulation with eight replicas and a temperature range of 280 to 600 K with heating for 1 ps, sampling at different temperatures for 1 ps and quenching to 280 K for 2.4 ps. During the folding simulation the peptide at the C-terminus of chain A reoriented by external restraints into a position, which permitted a later closing of the disulphide bond to chain D and the formation of the oxidized homotetramer. Therefore, we pulled the Cys504 to the place of the disulphide bond via constant force of 10 kcal/ (mol·Å) (0.7 nN) and then restrained the displacement of Cys504 with 500 kcal/ (mol·Å) out of this environment for a total of 66 ns per replica. During the last 330 ps the system relaxed shortly.

After relaxation we determined one structure of the 16 replica with both, the highest count of helical structure elements (like our previous publication indicated[2]), and the Cys504 in a position that enables disulphide bond formation. We connected a copy of the 41 aa at the C-terminus of this replica to each monomer, obtaining a CRMP2 homotetramer with four C-termini with 41 additional residues each. As a result, we got an extended structure of 518 aa per monomer (Arg16-Val531) (**Figure SI 1.A)**.

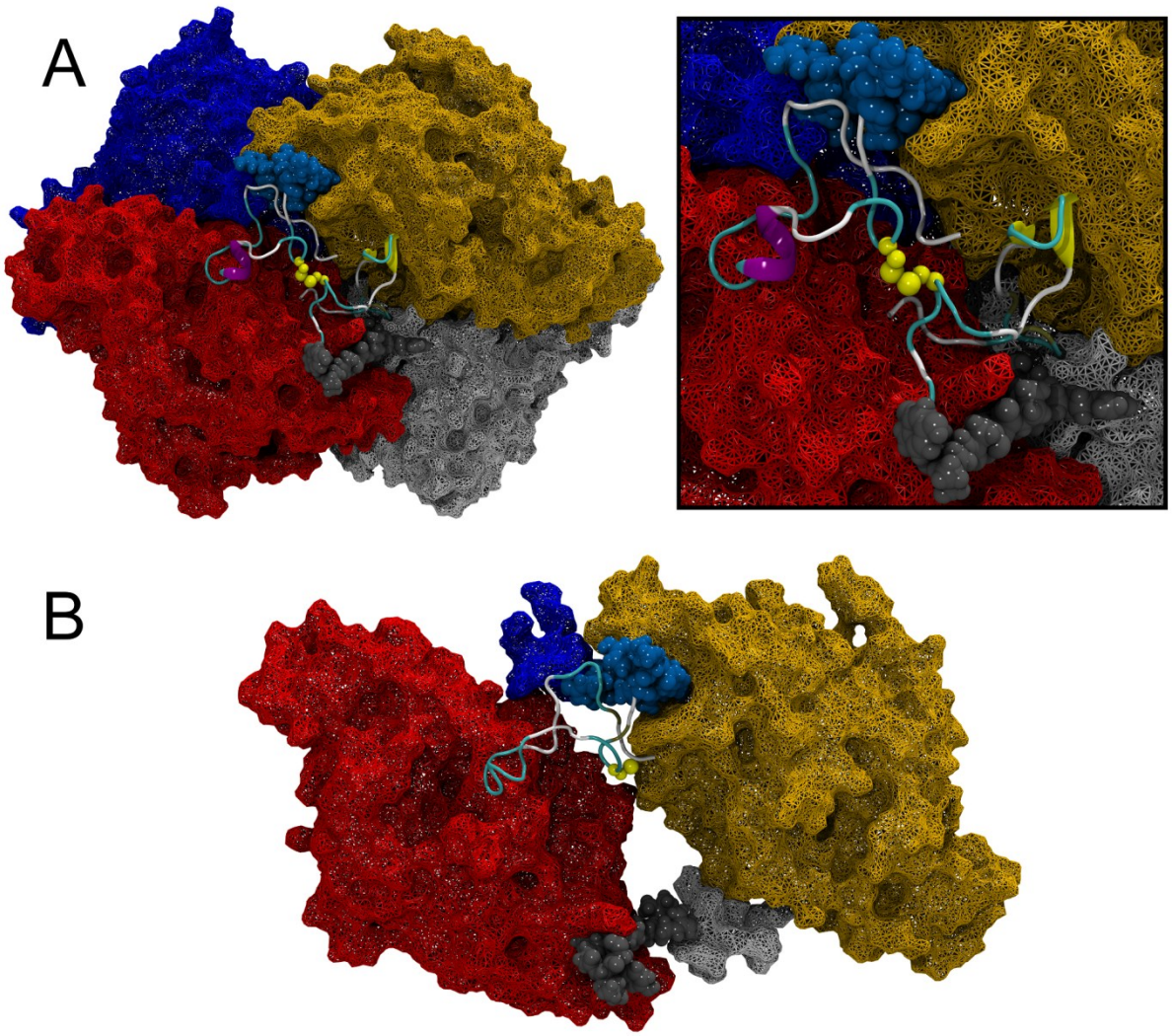

Figure SI 1: Steric view of CRMP2:

(A) **Snapshot of the oxidized CRMP2 homotetrameric structure. The four monomers are distinguished by colours (blue, red, yellow, and grey respectively). The mesh surface is based on the experimental crystal structure[1,32]. The monomers are extended by 41 amino acids at each C-terminus. The fragment with nine amino acids from the homology search is shown as van der Waals surface in colours related to the respective monomer (blue or grey, respectively). The structure of the remaining C-terminus fragment with 32 amino acids is presented with secondary structure elements (helix: purple and blue; sheet: yellow arrows; turn: cyan; coil: white) (cf. Table 1 in paper text). The Cys504 residues form the disulphide bonds (ball-and-stick, yellow).**

(Insert to A) **Magnification of in to the disulphide bond between the Cys504 residues of chain A (blue) and D (grey).**

(B) **Protein fragment for TIGER2 calculations of the peptide at the C-terminus as cut from similar structure as in** (A).

Homotetrameric CRMP2

In the reduced structures, the cysteine 504 residues of each subunit have protonated side chains. An oxidized structure was generated by connecting the final cysteine residues (504) of each two adjacent monomers. Two cysteine bridges between monomer 1 (chain A) and 4 (chain D) and between 2 and 3 (chains: B and C) (**Figure SI 1.A**) were formed.

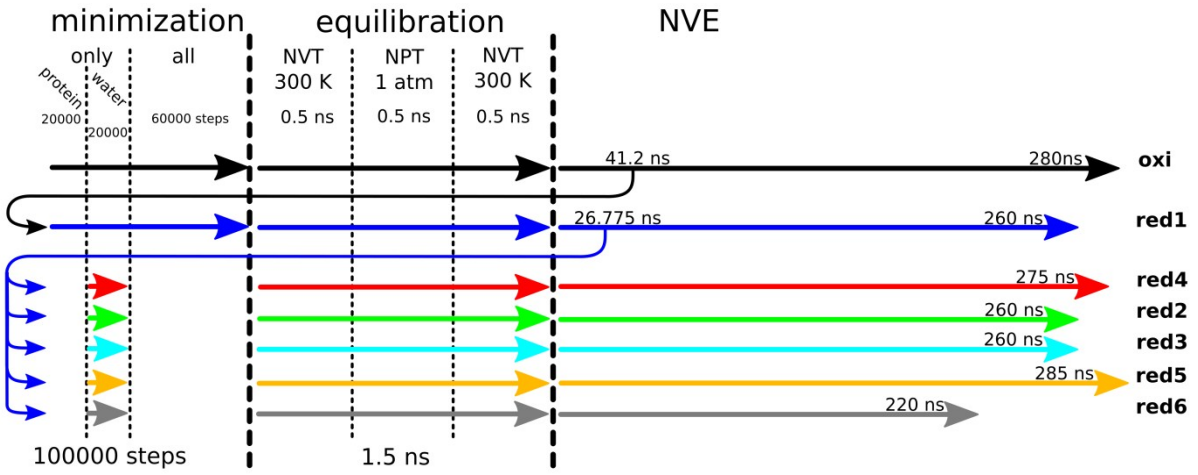

Figure SI 2: Schematic overview of simulations with the full CRMP2 molecules (oxi, red1 to red6):

Energy minimization of the system with water fixed in the box for 20000 steps, with the protein fixed for 20000 steps, with all atoms free for 60000 steps.

Molecular dynamics simulations for thermal equilibration: Heating up to 300 K, NPT run at 1 atm and 300 K, a second heating to 300 K for 500 ps respectively, NVE production runs for analysis.

Arrows indicate the flow of the simulation: originated red1 from the structure of oxi at 41 ns, with changes to the oxidized Cys504 and a new water box (plus counter ions). red2-red6 results of the structure of red1 at 27 ns, but with a new water box each and adapted concentrations of bivalent and counter ions.

The homotetramers have negative charges of -13 e per monomer, or totally -52 e. We aimed at reproducing the *in vitro* solutions from Stenmark et al. and Majava et al.[1,32] and performed simulations with 4 Ca^{2+}- ions (1.6 mM) in the oxidized and reduced states, and with 0 mM, 20 mM and 200 mM Ca^{2+} or Mg^{2+}-ions in the reduced state only. The four bivalent ions given from the crystal structure were at the same position in the protein structures[1,32] in all simulations, except for 0 mM. Excessive ions were distributed by xleap, an AMBER-tool[11,12]. The resulting total negative or positive charges of the system were compensated by monovalent Na^+ or Cl^- counter ions, respectively (see **Table 1** in paper text). The first simulation was the oxidized state with 4 Ca^{2+}-ions. After around 41 ns in NVE, we used a snapshot of its structure to build the reduced state by restoring the thiol groups of the Cys504 residues. The

structure of this state after around 27 ns in NVE was used for the simulations with other bivalent cation concentrations (**Figure SI 2**).

All systems were subjected to an energy minimization of 20000 steps, or 100000 steps for the calculations with 4 Ca^{2+}-ions, before MD simulations were performed. Equilibration simulations consisted of three parts, NVT, NPT and another NVT for 0.5 ns each. The NVE calculations, with scanning times of 200-300 ns at temperatures around 300 K, were used for further analyses.

Recombinant expression and purification of CRMP2

For recombinant protein expression, E. coli cells were propagated in a 3 l conical flask. The LB-medium (400 ml), containing the selective antibiotics, was inoculated at 37 °C with 2 % of an overnight culture of E. coli BL21 (DE3) codon-plus (Life technologies) harbouring the pET15b-CRMP2. At OD 0.6, expression was induced by addition of 0.5 mM IPTG (isopropyl-β-D-thiogalactopyranoside) and by lowering the temperature to 10 °C. The cells were harvested after 24 hours by centrifugation. Bacteria were lysed by incubation with 1 mg/ml lysozyme and 0.05 mg/ml DNase I for 20 minutes at room temperature (RT) and subsequent ultrasonic treatment for 2-times 2.5 minutes, 75 % intensity, 0.5 s cycle time (50 % cycling) using a Sonopuls HD2070 ultrasonic processor (Bandelin, Berlin, Germany). Recombinant His-tagged CRMP2 was purified by immobilized metal affinity chromatography using an Äkta FPLC system as suggested by the manufacturer (GE healthcare, Buckinghamshire, UK) at 4 °C.

CD spectroscopy

Circular dichroism spectra were recorded in a Jasco 810 instrument (Tokyo, Japan). Freshly purified CRMP2 was reduced with 5 mM DTT (dithiotreithol), 5 mM pH-neutralized TCEP (tris(2-carboxyethyl)phosphine), and 0.8 µM human Grx2c (glutarexdoxin 2)[2] for 30 minutes at RT. To remove all reductants, the protein solution was re-buffered using NAP-5 columns (GE healthcare). Next, the protein was oxidized by 200 µM H_2O_2 for 30 minutes at RT. H_2O_2 was removed by re-buffering in 10 mM KPO_4 buffer including 20 mM $MgCl_2$ at pH 7.4 as before. The oxidized sample (6 µM) was analysed in a 1 mm cuvette, scanning 0.2 nm steps, averaging 10 iterations. Subsequently, the protein was oxidized by addition of 1 mM H_2O_2 and incubated for 30 minutes at RT and analysed again. All spectra were corrected by subtraction of the respective baselines.

Differential scanning fluorimetry (thermofluor assay[33])

The thermal stability of reduced and oxidized CRMP2 was studied using the thermofluor assay as outlined in ref.[33]. 10 µM protein was reduced and oxidized as outlined above and re-buffered in 10 mM HEPES (2-[4-(2-hydroxyethyl)piperazin-1-yl]ethane sulfonic acid) pH 8, containing either 300 mM $MgCl_2$ or $CaCl_2$. Immediately after the starting temperature of 10 °C was reached, EDTA was added to adjust the concentrations of the ions to 0, 1.6, 20, or 200 mM Ca^{2+} or Mg^{2+}. SYPRO Orange was added (1:100 diluted, Sigma-Aldrich) and triplicates of the samples were heated in a CFX96 Real Time System from BioRad in 0.5 K increments from 10 to 100 °C. The increase in fluorescence due to binding of the dye to hydrophobic regions exposed during heating of the samples was recorded using the instrument's "FRET" settings.

Fluorescence spectroscopy

Time dependent quenching of tryptophan fluorescence was measured using a LS50B Fluorimeter (PerkinElmer, Boston, MA, USA). Recombinant CRMP2 was reduced with 5 mM DTT, 5 mM pH-neutralized TCEP for 30 minutes at RT. To remove all reductants, the protein solution was re-buffered in PBS (phosphate buffer saline) containing 20 mM $MgCl_2$ using NAP-5 columns (GE healthcare). 3 µM CRMP2 were used to measure the tryptophan fluorescence after excitation at a wavelength of 296 nm. The protein was oxidized using 1 mM H_2O_2 and the fluorescence quenching was recorded every 5 minutes.

We assumed second order kinetics in the pseudo first order limit, and derived rate constants k of the oxidation reaction according to equation * MERGEFORMAT (1) (see in following derivation):

$$\ln\left(\frac{F_r - F_o}{F_{t=x} - F_o}\right) = k\left([H_2O_2]_{t=0} - [P]_{t=0}\right)t \qquad \text{* MERGEFORMAT (1)}$$

We calculated first order rates $k\left([H_2O_2]_{t=0} - [P]_{t=0}\right)$ by a linear regression of the left hand expression in * MERGEFORMAT (1) against the time t. The ordinate values are the natural logarithms of the maximum difference between the fluorescence intensities F_r and F_o of fully reduced and oxidized proteins, respectively, over the difference between the fluorescence $F_{t=x}$ at t=x and F_o. Division of the slope by the difference of initial concentrations of H_2O_2, $[H_2O_2]_{t=0}$ and the reduced protein $[P]_{t=0}$ yields the second order rate constant k. At our conditions, $[P]_{t=0}$ is negligible with respect to the initial hydrogen peroxide concentration.

Derivation of pseudo first order kinetics for the quenching of the Trp295 fluorescence

The oxidation of any given protein or protein complex by hydrogen peroxide follows a second order reaction:

$$P_r + H_2O_2 \rightarrow P_o + H_2O_2$$

(P_r: reduced protein, P_o: oxidized protein)

The reaction rate can be calculated as expressed in equation * MERGEFORMAT (2):

$$-\frac{\delta[P_o]}{\delta t} = \frac{\delta[P_r]}{\delta t} = -k[P_r][H_2O_2] \qquad \text{* MERGEFORMAT (2)}$$

The concentrations of the reactants at t=x may also be expressed as follows:

$$[P_r] = [P_r]_{t=0} - [P_o]$$
$$[H_2O_2] = [H_2O_2]_{t=0} - [P_o]$$

The reaction rate can thus be expressed as:

$$-\frac{\delta[P_o]}{\delta t} = -k([P_r]_{t=0} - [P_o])([H_2O_2]_{t=0} - [P_o]) \qquad \text{* MERGEFORMAT (3)}$$

$$\Leftrightarrow \frac{\delta[P_o]}{([P_r]_{t=0} - [P_o])([H_2O_2]_{t=0} - [P_o])} = k\delta t \qquad \text{* MERGEFORMAT (4)}$$

$$\Rightarrow \int_0^{[P_o]} \frac{\delta[P_o]}{([P_r]_{t=0} - [P_o])([H_2O_2]_{t=0} - [P_o])} = k\int_0^t \delta t \qquad \text{* MERGEFORMAT (5)}$$

Integration using the method of partial fractions:

$$\Rightarrow \frac{1}{[H_2O_2]_{t=0} - [P_r]_{t=0}}\left(\ln\left(\frac{[P_r]_{t=0}}{[P_r]_{t=0} - [P_o]}\right) - \ln\left(\frac{[H_2O_2]_{t=0}}{[H_2O_2]_{t=0} - [P_o]}\right)\right) = kt \qquad \text{* MERGEFORMAT (6)}$$

$$\Leftrightarrow \frac{1}{[H_2O_2]_{t=0} - [P_r]_{t=0}}\ln\left(\frac{[H_2O_2][P_r]_{t=0}}{[P_r][H_2O_2]_{t=0}}\right) = kt \qquad \text{* MERGEFORMAT (7)}$$

$$\Leftrightarrow \ln\left(\frac{[H_2O_2][P_r]_{t=0}}{[P_r][H_2O_2]_{t=0}}\right) = k([H_2O_2]_{t=0} - [P_r]_{t=0})t \qquad \text{* MERGEFORMAT (8)}$$

Since the concentration of H_2O_2 greatly exceeds the concentration of P_r, the concentrations of $[H_2O_2]_{t=0}$ and $[H_2O_2]_{t=x}$ are essentially equal and the fraction on the left site can be reduced as follows:

$$\Rightarrow \ln\left(\frac{[P_r]_{t=0}}{[P_r]}\right) = k([H_2O_2]_{t=0} - [P_r]_{t=0})t \qquad \text{* MERGEFORMAT (9)}$$

Using Trp fluorescence quenching at the emission of 340 nm, $[P_r]_{t=0}$ and $[P_r]$ at t=x can be expressed as:

$$[P_r]_{t=0} \propto F_r - F_o$$
$$[P_r] \propto F_{t=x} - F_o$$

While F_r is the fluorescence of the reduced protein and F_o of the oxidized one. Equation * MERGEFORMAT (9) can thus be expressed as:

$$\Rightarrow \ln\left(\frac{F_r - F_o}{F_{t=x} - F_o}\right) = k_g\left([H_2O_2]_{t=0} - [P_r]_{t=0}\right)t \quad \text{* MERGEFORMAT (10)}$$

Thus, equation * MERGEFORMAT (10) can be used for linear regression of a plot of the natural logarithm of the maximal difference between the fluorescence of fully reduced and fully oxidized protein over the difference between the fluorescence at t=x and the fluorescence of the fully oxidized protein, against the time. The rate constant can now be calculated from the slope of the curve.

Results

Exposure of surfaces to solvent

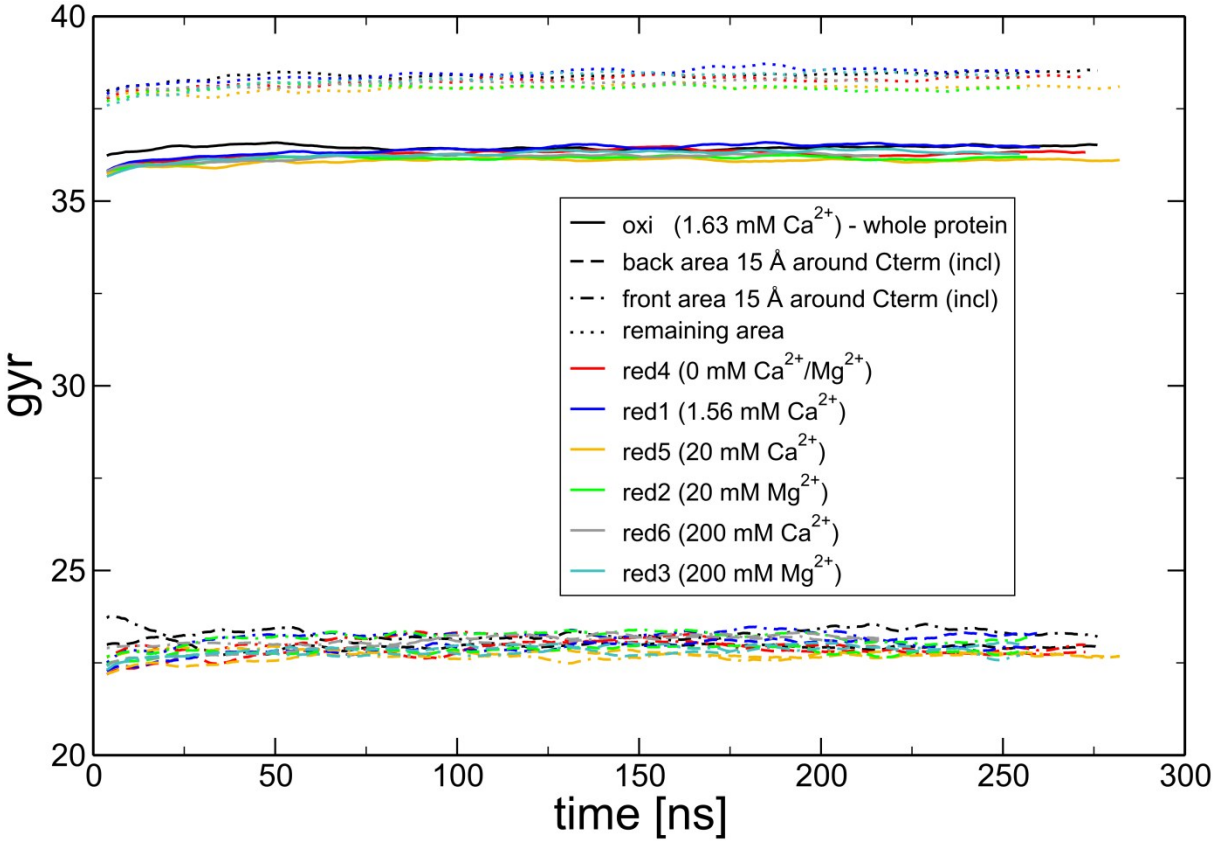

Figure SI 3: Gyradius of CRMP2 homotetramer as a function of time from the MD simulations: Oxidized with four structure stabilizing bivalent ions (black), reduced without any bivalent ions (red), with four structure stabilizing bivalent ions (blue), with 20 mM (Mg^{2+} green, Ca^{2+} yellow) and with 200 mM bivalent ions (Mg^{2+} cyan, Ca^{2+} grey). The full lines depict the whole protein, the broken lines only the area around C-termini (including them) with a maximal distance of 15 Å (separated to front- and backside), and the dotted line the remaining protein. The curves are running averages of the raw data with a window of 7.5 ns.

Correlation of Trp295 fluorescence wavelength and electrostatic energies for oxidized and reduced state

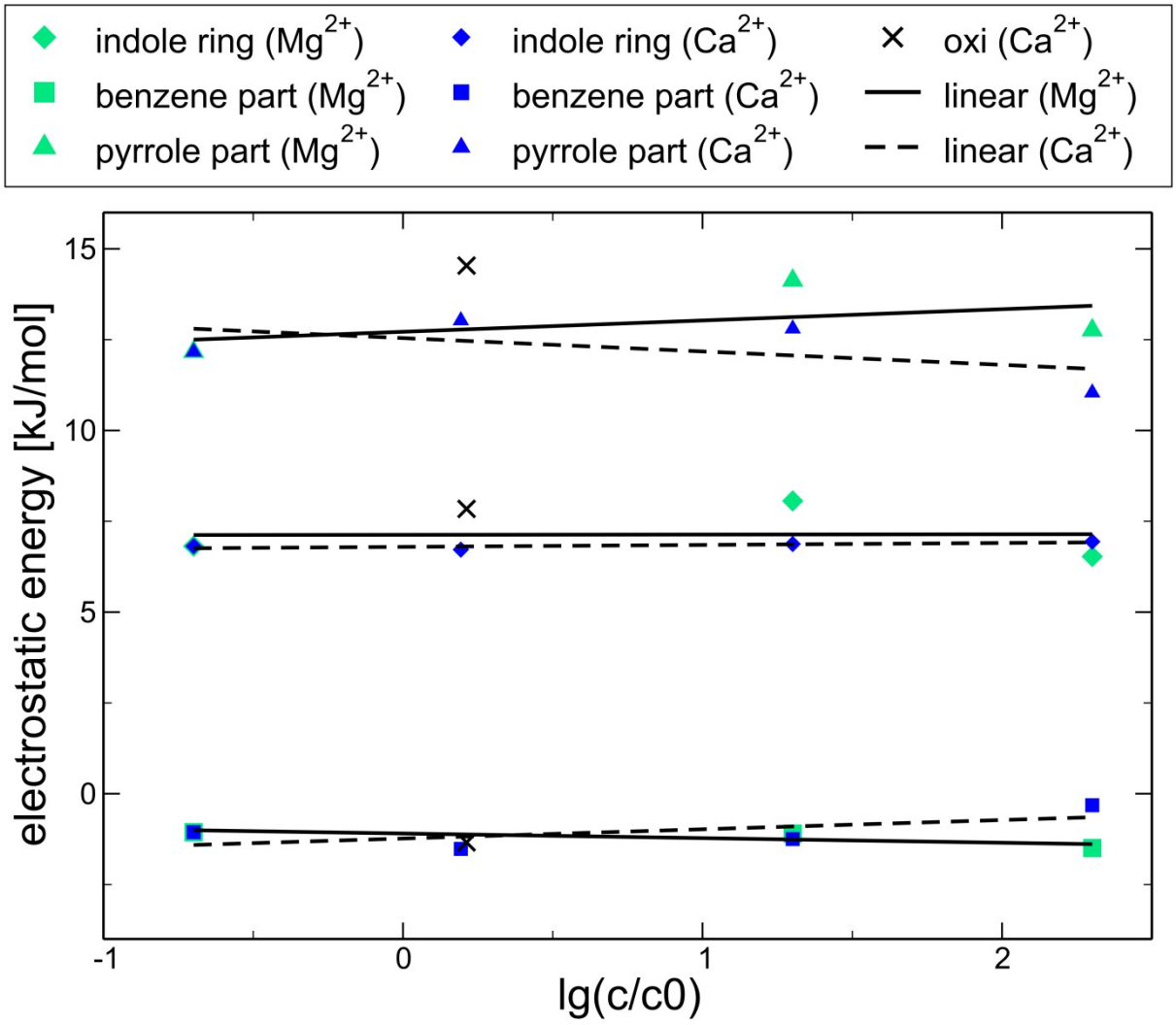

Figure SI 4: Electrostatic energy of components of the side chain of the Trp295 in the oxidized molecule (x) and at several ionic concentrations for the reduced state (coloured symbols). Components are the indole ring, and its benzene and pyrrole parts. The electrostatic energy in kJ/mol was averaged over the four Trp295 residues and over 30 frames with a 0.5 ns stride.

References

1. V. Majava, N. Loytynoja, W. Q. Chen, G. Lubec and P. Kursula, *The FEBS journal*, 2008, **275**, 4583-4596.
2. M. Gellert, S. Venz, J. Mitlöhner, C. Cott, E.-M. Hanschmann and C. H. Lillig, *Journal of Biological Chemistry*, 2013, **288**, 35117-35125.
3. Y. Gu, N. Hamajima and Y. Ihara, *Biochemistry*, 2000, **39**, 4267-4275.
4. N. Yamashita, T. Ohshima, F. Nakamura, P. Kolattukudy, J. Honnorat, K. Mikoshiba and Y. Goshima, *The Journal of Neuroscience*, 2012, **32**, 1360-1365.
5. K. Arnold, L. Bordoli, J. Kopp and T. Schwede, *Bioinformatics*, 2006, **22**, 195-201.
6. D. T. Jones, *Journal of Molecular Biology*, 1999, **292**, 195-202.
7. J. J. Ward, J. S. Sodhi, L. J. McGuffin, B. F. Buxton and D. T. Jones, *Journal of Molecular Biology*, 2004, **337**, 635-645.
8. E. M. Zdobnov and R. Apweiler, *Bioinformatics*, 2001, **17**, 847-848.
9. M. Welin, Karlberg, T., Andersson, J., Arrowsmith, C.H., Berglund, H., Busam, R.D., Collins, R., Dahlgren, L.G., Edwards, A.M., Flodin, S., Flores, A., Graslund, S., Hammarstrom, M., Herman, M.D., Johansson, I., Kallas, A., Kotenyova, T., Lehtio, L., Moche, M., Nilsson, M.E., Nyman, T., Persson, C., Sagemark, J., Svensson, L., Thorsell, A.G., Tresaugues, L., Van Den Berg, S., Weigelt, J., Wikstrom, M., Nordlund, P., Human Dihydropyrimidinase, http://www.rcsb.org/pdb/explore/explore.do?structureId=2vr2, DOI: http://dx.doi.org/10.2210/pdb2vr2/pdb).
10. J. C. Phillips, R. Braun, W. Wang, J. Gumbart, E. Tajkhorshid, E. Villa, C. Chipot, R. D. Skeel, L. Kalé and K. Schulten, *Journal of Computational Chemistry*, 2005, **26**, 1781-1802.
11. D. A. D. Case, T.A.; Cheatham III, T.E. ; Simmerling, C.L.; Wang, J.; Duke, R.E.; Luo, R.; Walker, R.C.; Zhang, W.; Merz, K.M.; Roberts, B.; Hayik, S.; Roitberg, A.; Seabra, G.; Swails, J.; Goetz, A.W.; Kolossváry, I.; Wong, K.F.; Paesani, F.; Vanicek, J.; Wolf, R.M.; Liu, J.; Wu, X.; Brozell, S.R.; Steinbrecher, T.; Gohlke, H.; Cai, Q.; Ye, X.; Wang, J.; Hsieh, M.-J.; Cui, G.; Roe, D.R.; Mathews, D.H.; Seetin, M.G.; Salomon-Ferrer, R.; Sagui, C.; Babin, V.; Luchko, T.; Gusarov, S.; Kovalenko, A.; Kollman, P.A., *Journal*, 2012.
12. P. Li, L. F. Song and K. M. Merz, *Journal of chemical theory and computation*, 2015, **11**, 1645-1657.
13. S. E. Feller, Y. Zhang, R. W. Pastor and B. R. Brooks, *The Journal of Chemical Physics*, 1995, **103**, 4613-4621.
14. G. J. Martyna, D. J. Tobias and M. L. Klein, *The Journal of Chemical Physics*, 1994, **101**, 4177-4189.
15. A. Aksimentiev and K. Schulten, *Biophysical Journal*, 2005, **88**, 3745-3761.
16. J. Eargle, D. Wright and Z. Luthey-Schulten, *Bioinformatics*, 2006, **22**, 504–506.
17. D. Frishman and P. Argos, *Proteins: structure, function and genetics*, 1995, **23**, 566–579.
18. W. Humphrey, A. Dalke and K. Schulten, *Journal of Molecular Graphics*, 1996, **14**, 33–38.
19. M. Sanner, A. Olsen and J.-C. Spehner, in *Proceedings of the 11th ACM Symposium on Computational Geometry*, ACM, New York, 1995, pp. C6-C7.
20. J. Stone, *An Efficient Library for Parallel Ray Tracing and Animation*, 1998.
21. A. Varshney, F. P. Brooks and W. V. Wright, *IEEE Computer Graphics and Applications*, 1994, **14**, 19–25.
22. A. Onufriev, D. Bashford and D. A. Case, *Proteins: Structure, Function, and Bioinformatics*, 2004, **55**, 383-394.
23. D. E. Tanner, K. Y. Chan, J. C. Phillips and K. Schulten, *Journal of chemical theory and computation*, 2011, **7**, 3635-3642.
24. D. E. Tanner, J. C. Phillips and K. Schulten, *Journal of chemical theory and computation*, 2012, **8**, 2521-2530.
25. J. Weiser, P. S. Shenkin and W. C. Still, *Journal of Computational Chemistry*, 1999, **20**, 217-230.
26. W. L. Jorgensen, J. Chandrasekhar, J. D. Madura, R. W. Impey and M. L. Klein, *The Journal of Chemical Physics*, 1983, **79**, 926-935.
27. D. J. Earl and M. W. Deem, *Physical Chemistry Chemical Physics*, 2005, **7**, 3910-3916.
28. Y. Sugita and Y. Okamoto, *Chemical Physics Letters*, 1999, **314**, 141-151.
29. Y. M. Rhee, E. J. Sorin, G. Jayachandran, E. Lindahl and V. S. Pande, *Proceedings of the National Academy of Sciences of the United States of America*, 2004, **101**, 6456-6461.
30. X. Li, R. A. Latour and S. J. Stuart, *The Journal of Chemical Physics*, 2009, **130**, -.
31. W. J. Menz, M. J. Penna and M. J. Biggs, *Computer Physics Communications*, 2010, **181**, 2082-2085.

32. P. Stenmark, D. Ogg, S. Flodin, A. Flores, T. Kotenyova, T. Nyman, P. Nordlund and P. Kursula, *Journal of neurochemistry*, 2007, **101**, 906-917.
33. F. H. Niesen, H. Berglund and M. Vedadi, *Nat. Protocols*, 2007, **2**, 2212-2221.